Available online at www.eccomasproceedia.org
Eccomas Proceedia SMART (2023) 95-106

ECCOMAS
Proceedia

X ECCOMAS Thematic Conference on Smart Structures and Materials
SMART 2023
D.A. Saravanos, A. Benjeddou, N. Chrysochoidis and T. Theodosiou (Eds)

FINITE ELEMENT ANALYSIS OF GUIDED WAVES IN FIBER METAL LAMINATES WITH DELAMINATIONS

WENDWOGA FULGENCE NIKIEMA[*1†], **NATALIE RAUTER**[*2], **AND ROLF LAMMERING**[*3]

[*]Institute of Mechanics
Helmut Schmidt University / University of the Federal Armed Forces
Holstenhofweg 85, 22043 Hamburg, Germany
e-mail: nikiemaw@hsu-hh.de[1†], natalie.rauter@hsu-hh.de[2], rl@hsu-hh.de[3]
web page: https://www.hsu-hh.de/

Abstract. The present work deals with the numerical analysis of the propagation of guided ultrasonic waves (GUW) in fiber-metal laminates (FML) and the effects resulting from their interaction with interlaminar damage. For this purpose, a numerical simulation including delaminations at different positions between layers is performed. FML is a hybrid material consisting of stacked layers of metal (e.g. steel) and fiber-reinforced polymer (FRP) and has been increasingly used in aerospace and lightweight construction over the past decade. In the context of Structural Health Monitoring (SHM), this novel material is still insufficiently explored in the case of damage detection using GUW. In the context of our work, it is of interest to investigate the different phenomena occurring during the interaction of the wave with the delamination and to formulate precise statements about its influence on the wave propagation. To explore the phenomena, three different models were considered: a defect-free model without delamination and two models with symmetrically and off-center located delamination, respectively. The simulation in this work is limited to a two-dimensional model, where the delamination is geometrically generated by de-merging the interface between the layers. In this case it is zero-thickness delamination. Moreover, the excitation is mode-selective and the investigated frequencies are in the range of fundamentally symmetric and antisymmetric modes. Thus, it is possible to consider the influence of the two modes separately. For the evaluation of the results different aspects were analyzed. First, the comparison of B-scans-representation show effects such as reflection, transmission and mode conversion when the guided wave hits the corners of the delamination. Furthermore, a singular phenomenon known as ”trapped mode” is clearly observed, where the mode-converted wave remains confined within the delamination area. Finally, the comparison of the displacement fields across the thickness before, in, and after delamination shows that the wave continues to propagate over the entire thickness instead of separating into two independent waves shapes.

Key words: guided ultrasonic waves, fiber metal laminates, delaminations, finite element method, displacement field, trapped wave, mode conversion.

[†] corresponding author

Peer-review under responsibility of the organizing committee of SMART 2023.
doi: 10.7712/150123.9768.445534

1 INTRODUCTION

In recent years, there has been a growing interest in utilizing elastic wave propagation for structural health monitoring of various structures. This approach offers the advantage of detecting damage at an early stage of development, thereby reducing the risk of endangering the safety of the structure. This is particularly crucial in the aerospace industry where ensuring the structural integrity of components throughout their service life remains a significant challenge. Although Non-Destructive Evaluation (NDE) methods have been employed to achieve this challenge, their application to large composite structures is time-consuming. Consequently, current research is focused on the use of Guided Ultrasonic Waves (GUW) for damage detection, owing to their ability to propagate over a wide range with minimal amplitude attenuation [1, 2].

Fiber Metal Laminates (FML) are novel hybrid composite materials consisting of a stack of two types of layers of metal and Fiber-Reinforced Polymer (FRP). This combination offers a high strength-to-weight ratio, corrosion resistance, and ductility [3, 4]. However, identifying and characterizing defects such as delaminations, fiber breakage, or interlaminar detachments is crucial for ensuring safety [4]. GUW-based Structural Health Monitoring (SHM) is a method that has been analyzed for both isotropic materials and thin-walled structures made of FRP see [5, 6]. Assuming constant stiffness and density throughout its thickness, both cases exhibit the complex multi-modal behavior of Lamb waves, which was initially described by Horace Lamb [7]. Analytical solutions to these equations can be found in various textbooks, such as [8, 9, 10], for isotropic materials in [5, 11] and in [12, 13]. For single transversely-isotropic layers, orthotropic layers, and layered structures, adaptations can be found in [11, 14, 15, 16]. As GUW propagation is not only multi-modal but also highly dispersive, phase and group velocities vary with frequency [6], as shown in dispersion diagrams.The analysis and interpretation of displacement fields across the thickness of a laminate are crucial for understanding the interaction of propagating waves with internal damage in structures, making it a topic of significant interest in SHM. For FML, the high impedance difference between layers results in frequency-dependent characteristics in displacement fields [3].

In the present study, the behavior of GUW in FML with delaminations is investigated by numerical simulations. In order to gain insight into the physical processes, the finite element method is used. The structure under study and the numerical model are presented in the next chapter, followed by the presentation and analysis of the displacement fields under different representations. Finally, the study is concluded with a summary and an outlook on the next steps of research.

2 MATERIAL AND MODEL DESCRIPTION

In this work, the numerical investigation of GUW in FML was carried out using the commercial finite element software COMSOL Multiphysics. For this purpose, a two-dimensional model was developed corresponding to the FML plate studied in the research group.

2.1 Geometry

The considered model of FML consists of a plate with sixteen layers combining CFRP layers with thin steel foils. The layers are superimposed and have the following configuration: [steel / 0°_4 / steel / 0°_2]$_s$, see Fig. 1. The layer thicknesses differ minimally and are 0.10 mm for each steel foil and 0.125 mm for each CFRP layer. This gives a total laminate thickness of 1.9 mm. The total length of the FML extends to 0.75 m.

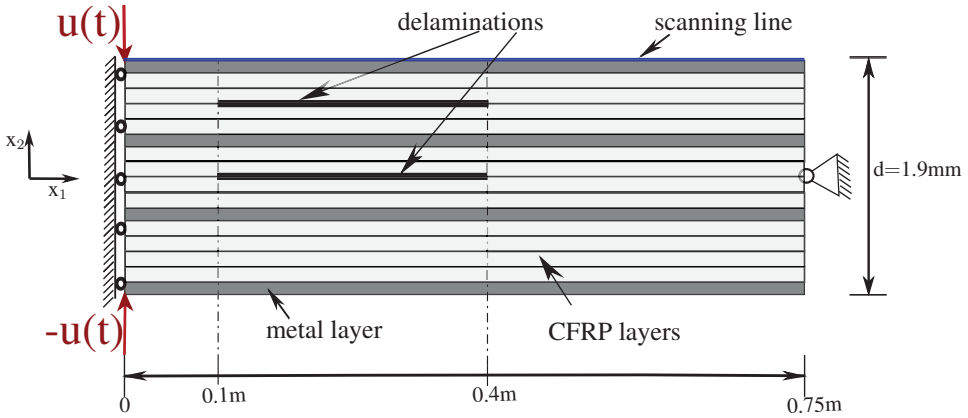

Figure 1: FML structure with two delaminations between layers 8 and 9 (center) and 3 and 4 (off-center), bearings at left and right edge, and displacement loads.

2.2 Material

The materials used in this work are steel 1.4310 and CFRP Hexply 8552-AS4 with the parameters listed in Table 1. When the stacking of the layers is closely examined, a high impedance jump between the layers of steel and CFRP is observed in the x_2-direction. These impedance jumps have an impact on the shape of the displacement fields, which will be presented in the next section.

Table 1: Material properties.

	E_{11} [GPa]	E_{22} [GPa]	G_{12} [GPa]	ν_{12} [-]	ν_{23} [-]	ρ [kg/m^3]
Steel 1.4310	180	180	69.2	0.30	0.30	7870
CFRP Hexply 8552-AS4	127.28	9.24	4.83	0.30	0.37	1580

2.3 Simulation setup

The simulation presented here uses quintic Lagrangian elements with 36 nodes per element. The calculation is performed in the time domain assuming a plane strain state. The FML struc-

ture is discretised for both steel and CFRP layers, with 1 element per layer throughout the thickness and 750 elements in the longitudinal direction. The simulation parameters can be found in Table 2. The structure depicted in Fig. 1 is subjected to a fixed bearing on the left side in the x_1-direction, while a fixed bearing is imposed in both directions at the center on the right side.

Table 2: Parameters of the 2D numerical simulation.

Parameter	**Value**	**Unit**
Element size steel	1.0×0.1	mm^2
Element size CFRP	1.0×0.125	mm^2
Number of elements in x_1-direction	750	[-]
Number of elements (per layer) in x_2-direction	1	[-]
quintic Lagrangian element	36	nodes
Model thickness	1.9	mm
Model length	750	mm
Excitation frequency	150	kHz

The focus of this study is on modeling delaminated areas, which are a type of interlaminar damage that can occur during manufacturing processes or due to low velocity impacts. In order to investigate the effect of delaminations on wave propagation, zero-thickness delaminations are modeled. To achieve this, nodes are split along the delamination length, resulting in two separate edges. The geometry is generated by dividing the layers above, below, and between the delaminations into three rectangular shapes, so that each section can be treated separately. Then, the appropriate function of the software package is applied to the middle edge to create the separation of the interfaces. Two different locations of delamination are considered, one in the center of the laminate and the other off-center placed. The delamination in the center is between layers 8 and 9, while the off-center delamination is between layers 3 and 4 above the centerline. Both modeled delaminations have a length of 300 mm and start at $x_1 = 0.1$ m, as shown in Fig. 1. The relatively long length of the delaminations compared to the total length of the laminate allows for a thorough analysis of the phenomena occurring within different kinds of delaminations, despite the high velocity of the fundamental mode waves.

2.4 Excitation

The FML structure undergoes displacement-controlled excitation using a five cycle Hanning windowed sine burst at a frequency of 150 kHz. To analyze the impact of the different fundamental wave modes on the defect, the laminate is subjected to symmetric and anti-symmetric loads separately. Mode-selective excitation is achieved by orienting the excitation function in the same direction for the antisymmetric mode and in the opposite direction for the symmetric mode, whereby the excitation occurs at the top and bottom corners of the left edge, as shown in Fig. 1.

3 Results and discussion

In this section, the numerical results are presented and discussed. For this purpose B-scans are utilized to display the wave propagation along the surface of the model over time. To conduct an analysis of these diagrams, the outcomes stemming from symmetric and antisymmetric excitation are evaluated individually. In each part of the plots, it is essential to compare the plots of centered and off-centered delamination with those without. Subsequently, it is also of interest to analyze and compare the shape of the displacement fields across the thickness at specific locations.

3.1 Interaction of the fundamental wave mode with delaminations using B-scans

Symmetric wave mode S_0

Fig. 2 (a) and 2 (b) show B-scans of an undisturbed propagation of the S_0 mode wave over the entire length with complete reflection at the right edge. Due to the larger amplitudes of the in-plane displacements compared to the out-of-plane displacements for the S_0 wave mode, the signal in Fig. 2 (a) is a more pronounced one than that in Fig. 2 (b).

The results for the delaminated structure show some differences as illustrated in Fig. 2 (c) and (d). When the wave front encounters the left edge of the delamination (blue vertical line at coordinate $x = 0.1$ m), three phenomena can be observed. First, the most part of the wave is transferred to the sublaminates and propagates along the delamination zone. Secondly, a small part of the wave is reflected in the opposite direction and finally, another segment of the S_0 wave mode converts into an A_0 wave mode and propagates towards the sublaminate. The B-scan shows a larger inclination because the A_0 wave mode has a lower velocity than the S_0 wave mode.

When the wave front hits the right edge of the delamination (vertical dashed line at coordinate $x = 0.4$ m), the same effects as transmission, reflection and mode conversion occur again. The transmitted and reflected waves propagate in the expected direction, but the converted wave mode propagates in the opposite direction. If the behaviour of the mode-converted wave is observed over a longer period of time, it can be seen that it remains trapped in the delamination zone. This phenomenon is described in the literature as "trapped mode" [4, 17], and the results presented there agree with those of the present work. Only the reflected or transmitted partial waves of the excitation mode can propagate over the entire laminate. When the S_0 wave mode encounters the off-center delamination (as depicted in Fig. 2 (e) and (f)), several effects are observed. These include the transmission and reflection of the main wave and the conversion of the wave into the A_0 wave mode. This mode propagates not only within the delaminated portion but also back into the undamaged area, allowing it to travel through the entire laminate [18]. The research has shown that by shifting the delamination halfway between the layers, similar results are obtained. This implies that the trapped mode phenomenon is exclusive to symmetrically placed defects. The phenomenon described above can be explained by the fact that the main laminate vibrates with a different eigenmode than the structure in the delamination zone. Thus, the corners of the delamination cause a total reflection of the converted mode over the

entire thickness and confine it to the delamination zone. For damage detection, this means that the damage is likely to be in the center of the laminate if the sensor only measures reflected or transmitted waves with the same mode as the excitation wave.

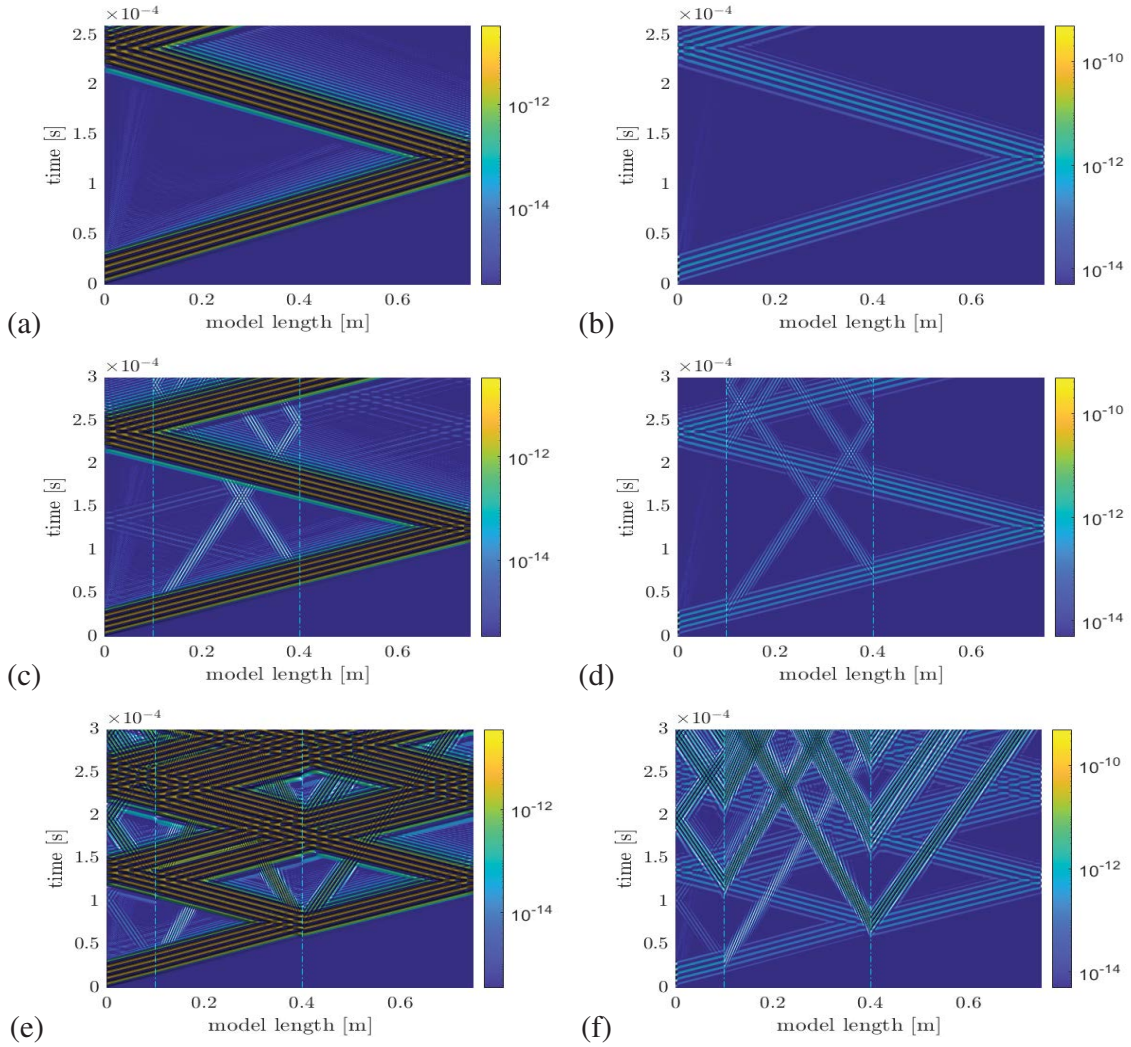

Figure 2: B-scans with displacement data in m of the S_0 wave propagation in FML at 150 kHz. Left: In-plane displacement, Right: Out-of-plane displacement. (a,b): without delamination, (c,d): symmetrically placed delamination, (e,f): off-center placed delamination.

Antisymmetric wave mode A_0

Fig. 3 (a) and (b) illustrate an undisturbed A_0 wave propagating along the entire plate and being completely reflected at the right outer edge, similar to the results of the previous section. The following Fig. 3 (c) and (d) show the results with symmetrically placed delamination. When the main wave hits the left corner of the delamination, the same effects occur as with the sym-

metrical waveform. Thus, the A_0 mode wave generates a converted S_0 mode wave that remains trapped in the delamination zone. The trapped mode phenomenon thus occurs in both symmetric and antisymmetric wave propagation. The results with off-center placed delamination

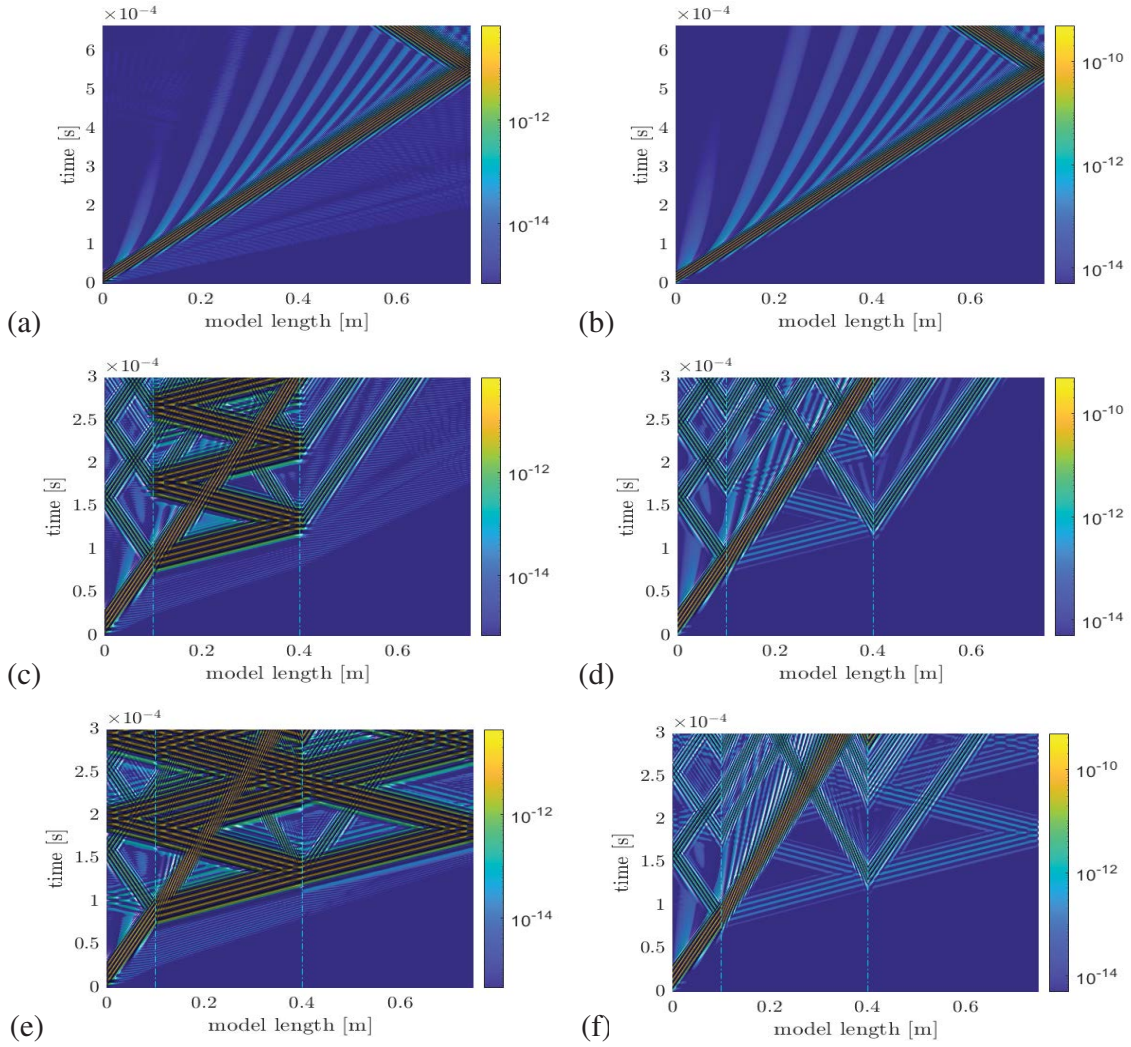

Figure 3: B-scans with displacement data in m of the A_0 wave propagation in FML at 150 kHz. Left: In-plane displacement, Right: Out-of-plane displacement. (a,b): without delamination (c,d) symmetrically placed delamination (e,f) off-center placed delamination.

(see Fig. 3 (e) and (f)) show the same behaviour as with symmetrical wave propagation. All the interactions mentioned in the previous part, such as transmission, reflection, and mode conversion, occur. The trapped mode phenomenon is also not observed, so that its existence is only confirmed for the case of symmetrically placed delamination. Finally, it can be observed that in all images of Fig. 3, but mainly in (a) and (b), slower waves with low amplitude (bright

curved stripes) are seen above the main wave. This phenomenon is due to the strongly dispersive behaviour of the A_0 wave, which does not occur with the S_0 wave (see pages 100, 101 of [19]).

3.2 Displacement fields over the thickness

This section deals with the comparison of the displacement fields across the thickness. The shape and amplitude of the propagating wave are analyzed to determine how delaminations placed at various positions affect them. To achieve this goal, it is crucial to understand the

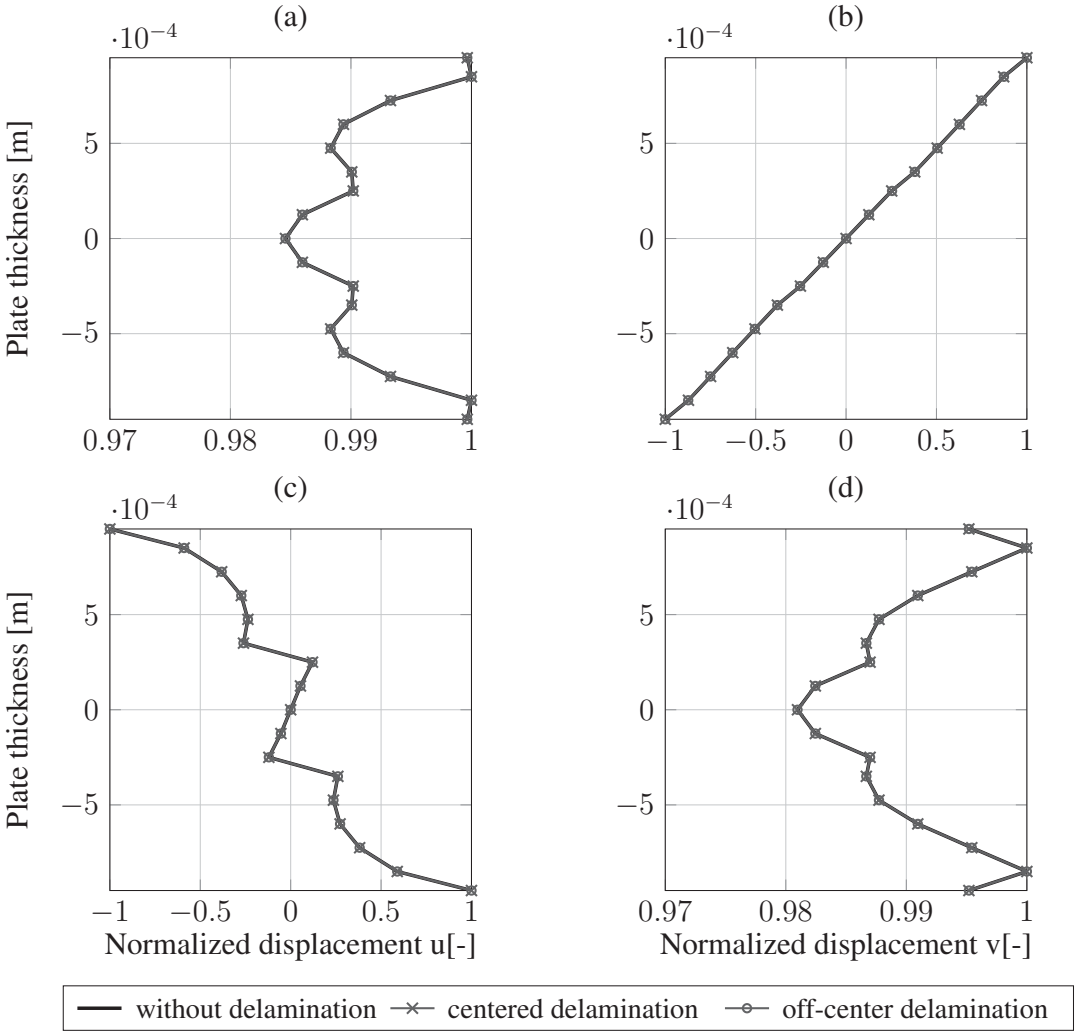

Figure 4: Normalized displacement field over the thickness in front of the delamination at $x = 50$ mm. Left side (a, c): in plane, right side (b, d): out of plane, top side (a, b): S_0 mode, bottom side (c, d): A_0 mode.

properties of waves in an FML without any defects, including their shape and amplitude, and

to make a quantitative and qualitative comparison of these properties with those including defects. Regarding the current research on wave propagation in FML, it can be concluded that the displacement field over the thickness has been well studied and validated analytically as well as numerically [3]. A direct comparison with the results discussed here show a qualitative agreement in the case of defect-free FML. For the following analysis, the shape of the normalized displacement fields before, in and after delamination in the FML-model without, with centered and off-center delamination are compared. Fig. 4 shows the in-plane (a, c) and out-of-plane

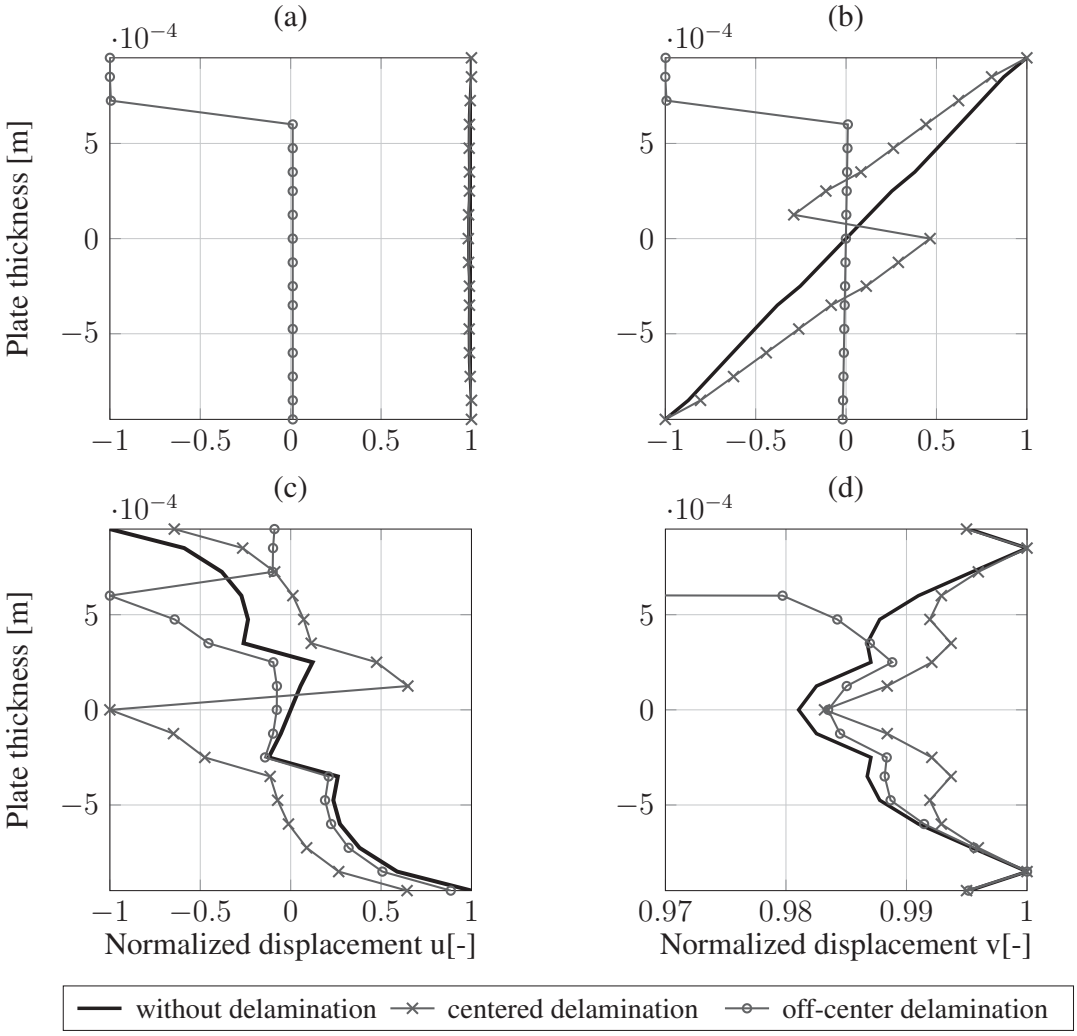

Figure 5: Normalized displacement field over the thickness in the center of the delamination at $x = 250$ mm. Left side (a, c): in plane, Right side (b, d): out of plane, Top side (a, b): S_0 mode, Bottom side (c, d): A_0 mode.

(b, d) components of the displacement fields in front of the delamination at coordinate $x = 50$ mm with symmetric (a, b) and antisymmetric (c, d) excitation. From the graphs, a qualitatively

perfect match can be seen in the shape of all simulated models. This is no longer the case when considering the displacement fields in the center of the delaminations at the coordinate $x = 250$ mm. In Fig. 5 it can be seen that there are differences in the shape of the displacement fields. Fig. 5 (a) and (b) show qualitatively consistent results for the cases without and with centered delamination, where (b) shows a zigzag in the middle, which is due to a clafing of the two interfaces. In the case of the FML with off-center delamination, the clafing is also observed, but

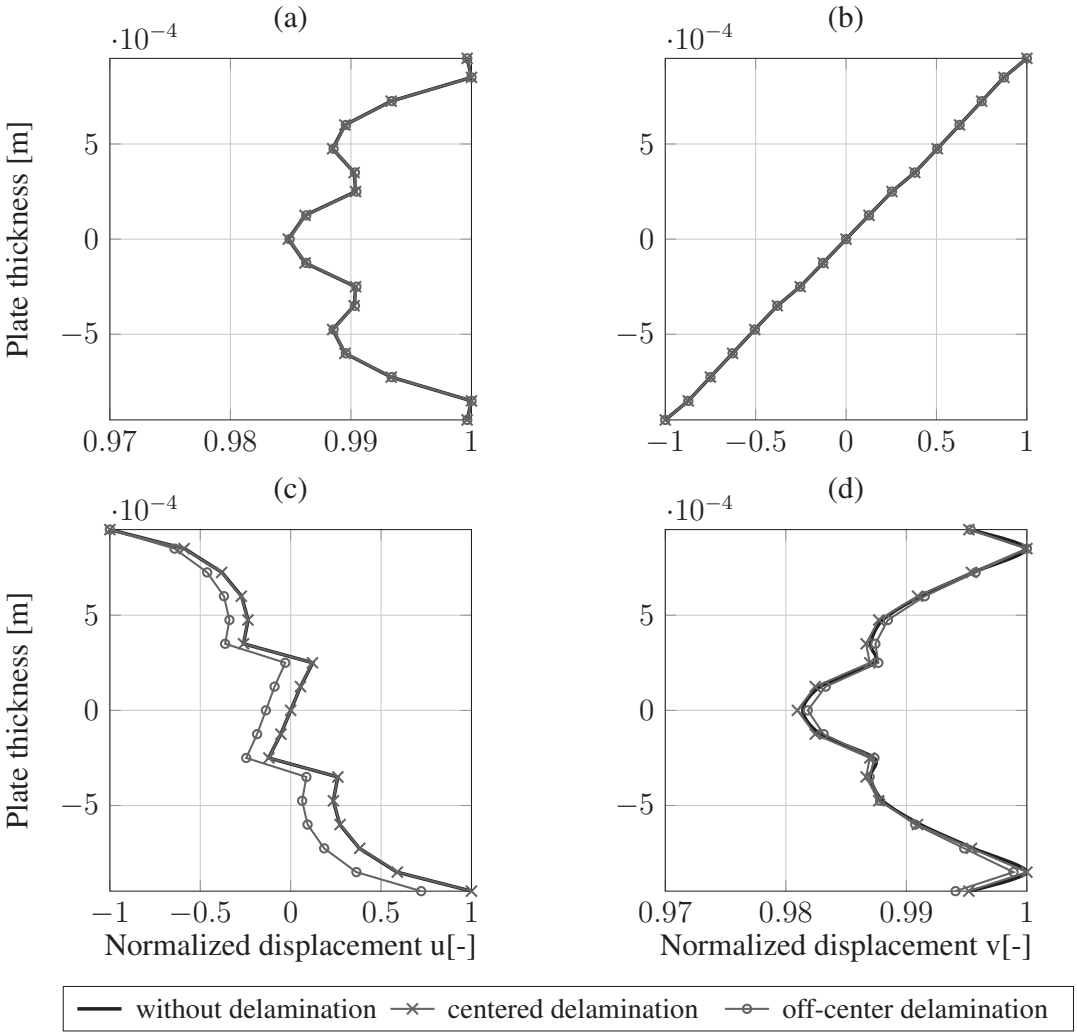

Figure 6: Normalized displacement field over the thickness after the delamination at $x = 550$ mm. Left side (a, c): in plane, Right side (b, d): out of plane, Top side (a, b): S_0 mode, Bottom side (c, d): A_0 mode.

with relatively higher absolute amplitudes. If the section below the delamination is considered, a similar shape is observed. Fig. 5 (c) and (d) show a good quality match of shape, with the clafing occurring in close proximity to the delamination. In addition, it can be mentioned that

the discrepancy in the amplitude sizes increases as one moves closer to the delamination zone.

Fig. 6 shows the comparison of the displacement fields after the delamination zone at coordinate $x = 550$mm. Fig. 6 (a) and (b) show a qualitative agreement of shape between the three models. However, for the antisymmetric excitation in (c) and (d), a small deviation in the amplitudes for the in-plane and out-of-plane components can be observed.

Finally, it can be seen from all the figures considered in this section that the shape of the displacement fields did not change significantly when a delamination is included and that the wave continues to propagate over the entire thickness and is not split into two partial waves.

4 CONCLUSION

The main objective of this study was to investigate the influence of defects such as delamination within an FML structure on GUW. The numerical results are valid for a frequency range of up to 250 kHz, in which only fundamental modes occur. The findings of this investigation serve to improve our understanding of the detection and characterisation of damage in FML. The observed trapped-mode phenomenon in symmetrically defined delaminations can also be found in other composite and isotropic materials. Furthermore, it can be seen that GUW preserves its standard shape symmetry throughout the thickness when crossing delaminations. A deep understanding of the displacement fields is important for other issues such as the interpretation of the sensor signals and the optimal placement of the sensor network. In further studies, the two-dimensional model will be extended to a three-dimensional model in order to compare the results and other types of defects such as fiber breakage and low velocity impact damage will be considered.

Acknowledgement The financial support within the Research Unit 3022 “Ultrasonic Monitoring of Fibre Metal Laminates Using Integrated Sensors”(project number: 418311604) by the Deutsche Forschungsgemeinschaft (DFG) is gratefully acknowledged.

REFERENCES

[1] W. Ostachowicz, P. Kudela, M. Krawczuk, and A. Zak, *Guided waves in structures for SHM: The time-domain spectral element method*. Chichester, West Sussex and Hoboken, NJ: Wiley, 2012.

[2] K. Ono, “Review on structural health evaluation with acoustic emission,” *Applied Sciences*, vol. 8, no. 6, p. 958, 2018.

[3] A. Mikhaylenko, N. Rauter, N. K. Bellam Muralidhar, T. Barth, D. A. Lorenz, and R. Lammering, “Numerical analysis of the main wave propagation characteristics in a steel-cfrp laminate including model order reduction,” *Acoustics*, vol. 4, no. 3, pp. 517–537, 2022.

[4] C. Ramadas, K. Balasubramaniam, M. Joshi, and C. V. Krishnamurthy, “Interaction of the primary anti-symmetric LAMB mode (A_0) with symmetric delaminations: numerical and experimental studies,” *Smart Materials and Structures*, vol. 18, no. 8, p. 085011, 2009.

[5] V. Giurgiutiu, *Structural health monitoring with piezoelectric wafer active sensors*. Amsterdam: Academic Press/Elsevier, 2008.

[6] R. Lammering, U. Gabbert, M. Sinapius, T. Schuster, and P. Wierach, Eds., *Lamb-wave based structural health monitoring in polymer composites*, ser. Research topics in aerospace. Cham: Springer, 2018.

[7] H. Lamb, "On waves in an elastic plate," *Proceedings of the Royal Society of London. Series A, Containing Papers of a Mathematical and Physical Character*, vol. 93, no. 648, pp. 114–128, 1917.

[8] I. A. Viktorov, *Rayleigh and Lamb waves: Physical theory and applications*, ser. Ultrasonic technology. New York: Springer Science + Business Media, 2013.

[9] J. D. Achenbach, *Wave propagation in elastic solids*, ser. North-Holland series in applied mathematics and mechanics. Amsterdam: North-Holland Pub. Co, 1973, vol. volume 16.

[10] K. F. Graff, *Wave motion in elastic solids*, 1st ed. New York: Dover Publ, 1991.

[11] J. L. Rose, *Ultrasonic guided waves in solid media*. New York, NY: Cambridge Univ. Press, 2014.

[12] A. R. Nandyala, A. K. Darpe, and S. P. Singh, "Effective stiffness matrix method for predicting the dispersion curves in general anisotropic composites," *Archive of Applied Mechanics*, vol. 89, no. 9, pp. 1923–1938, 2019.

[13] N. Vu Ngoc, "Zur Wellenausbreitung in geschichteten Faserverbundstrukturen unter Verwendung nichtlinearer Stoffgesetze," Dissertation, Helmut Schmidt University / University of the Federal Armed Forces Hamburg, Hamburg, 2020.

[14] A. H. Nayfeh, "The general problem of elastic wave propagation in multilayered anisotropic media," *The Journal of the Acoustical Society of America*, vol. 89, no. 4, pp. 1521–1531, 1991.

[15] S. I. Rokhlin and L. Wang, "Ultrasonic waves in layered anisotropic media: characterization of multidirectional composites," *International Journal of Solids and Structures*, vol. 39, no. 16, pp. 4133–4149, 2002.

[16] L. Wang and S. I. Rokhlin, "Ultrasonic wave interaction with multidirectional composites: modeling and experiment," *The Journal of the Acoustical Society of America*, vol. 114, no. 5, pp. 2582–2595, 2003.

[17] E. Glushkov, N. Glushkova, A. Eremin, and R. Lammering, "Trapped mode effects in notched plate-like structures," *Journal of Sound and Vibration*, vol. 358, pp. 142–151, 2015.

[18] C. Ramadas, K. Balasubramaniam, M. Joshi, and C. V. Krishnamurthy, "Interaction of guided lamb waves with an asymmetrically located delamination in a laminated composite plate," *Smart Materials and Structures*, vol. 19, no. 6, p. 065009, 2010.

[19] S. von Ende, "Transient angeregte LAMB-Wellen in elastischen und viskoelastischen Platten; Berechnung und experimentelle Verifikation," Dissertation, Helmut Schmidt University / University of the Federal Armed Forces Hamburg, Hamburg, 2008.